Electronic Supplementary Material (ESI) for New Journal of Chemistry.

Shape selectivity of zeolite for hydroisomerization of long-chain alkanes

Yuanlong Han,[a,b] Jiamin Yuan,[b,d] Mengjiao Xing,[a,b] Jian Cao,[a,b] Zhiqiang Chen,[a,b] Ling Zhang*[c] Zhichao Tao*[c] Zhiqiang Liu,[d] Anmin Zheng,[d] Xiaodong Wen,[a,c] Yong Yang,*[a,c] and Yongwang Li[a,c]

[a] *State Key Laboratory of Coal Conversion, Institute of Coal Chemistry, Chinese Academy of Sciences, Taiyuan 030001, PR China;*

[b] *University of Chinese Academy of Sciences, Beijing, 100049, PR China;*

[c] *National Energy Research Center for Clean Fuels, Synfuels China Co., Ltd., Beijing 101400, PR China.*

[d] *State Key Laboratory of Magnetic Resonance and Atomic and Molecular Physics, National Center for Magnetic Resonance in Wuhan, Key Laboratory of Magnetic Resonance in Biological Systems, Wuhan Institute of Physics and Mathematics, Innovation Academy for Precision Measurement Science and Technology, Chinese Academy of Sciences, 430071 Wuhan, China*

*To whom correspondence should be addressed.

E-mail: zhichaotao@163.com (Zhichao Tao); zhangling@synfuelschina.com.cn (Ling Zhang); yyong@sxicc.ac.cn (Yong Yang).

Keywords: hydroisomerization, long-chain alkanes, ZSM-12 zeolite, pore mouth catalysis, key lock catalysis

1. Reagents

All reagents were used as received without further purification in present study: silica sol (SiO_2 = 30 wt.%, Qingdao Haiyang Chemical Co., Ltd.), aluminum sulfate (99%, Sinopharm Chemical Reagent Co., Ltd.), sodium aluminate (98 wt.%, Tianjin Guangfu Fine Chemical Research Institute), potassium hydroxide (85 wt.%, Beijing Chemical Co., Ltd.), sodium hydroxide (96 wt.%, Beijing Chemical Co., Ltd.), 1,6-diaminohexane (99 wt.%, DAH, Sinopharm Chemical Reagent Co., Ltd.), Tetraethylammonium bromide (98 wt.%, TEABr, Shanghai Aladdin Biochemical Technology Co., Ltd.), hydrochloric acid (37 wt.%, Sinopharm Chemical Reagent Co., Ltd.), ammonium chloride (98 wt.%, Beijing Chemical Co., Ltd.), $H_2PtCl_6 \cdot 6H_2O$ (37 wt.%, Sinopharm Chemical Reagent Co., Ltd.), and de-ionized water.

2. Model and molecular dynamics simulation details

2.1. The calculation of the size of molecule

The length, width and height of a molecule are calculated from the difference between the maximum and the minimum coordinate of a molecule at each direction (*i.e.* x, y and z) [1]. In this work, the length, width and height are defined as formula (3) to (5). Xmax/Xmin (Ymax/Ymin or Zmax/Zmin) is the maximum/minimum coordinate of the atom inside the molecule at different directions. Corresponding schematic diagram for the definition of the molecular length, width and height is shown in Fig. S1.

$$Length = Xmax - Xmin \quad (3)$$

$$Width = Zmax - Zmin \quad (4)$$

$$Height = Ymax - Ymin \quad (5)$$

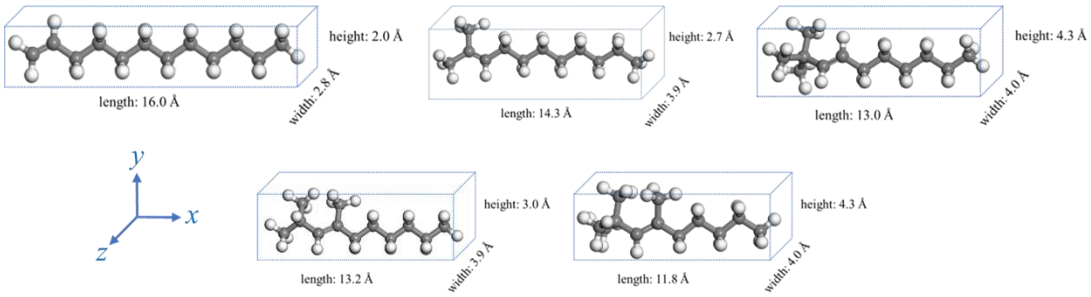

Fig. S1. Definition of the molecule length, width and height

2.2. Monte Carlo (MC) simulation

The initial framework was derived from International Zeolite Associations (IZA) database [2]. The 2 × 2 × 6, 2 × 10 × 4 and 2 ×2 × 5 supercell structure was selected for TON, MTW and MOR zeolite and optimized by GULP [3] with SLC [4] core-shell force field. In MC simulations, a Nosé-Hoover thermostat was adopted, the temperature was maintained at 25 ℃. The MC simulation was operated at 8, 16 and 8 loadings for TON, MTW and MOR zeolite (one molecule per channel). The simulation was equilibrated for 1×10^6 steps, followed by another 1×10^7 steps of production. All the interactions in this system were described by a widely used COMPASS force field [5].

2.3. Molecular dynamic (MD) simulations

The output structures of the MC simulation were used as the initial structure of the MD simulation. In the simulation, the COMPASS [5] force field was also applied in this system. A Nosé-Hoover thermostat

was employed, the temperature was set at 280 ℃ in NVT ensemble. The host-guest interactions were modeled by Lennard-Jones potential, with a cutoff radius 12.5 Å. All the simulations were equilibrated for 1 ns follow by 20 ns of statistics, with a time step of 1 fs. The trajectories of molecules were recorded every 1000 steps. For each system, independent MD simulations of 5 times was done to obtain a reliable result statistically. All MD simulations were conducted on the Materials Studio 7.0 with Forcite module.

2.4. Diffusion coefficient

Based on the MD simulations, the mean square displacement (MSD) of adsorbate was computed by the relation:

$$MSD(\tau) = \frac{1}{N_m} \sum_{i}^{N_m} \frac{1}{N_\tau} \sum_{t_0}^{N_t} [r_i(t_0 + \tau) - r_i(t_0)]^2 \qquad (1)$$

where N_m indicated the number of molecule and r_i referred to the location of the center of mass of molecule i. From Einstein relation [6], the self-diffusion coefficient, Ds, was calculated:

$$MSD(\tau) = 2nD_S\tau + b \qquad (2)$$

where n represented the framework dimension (n = 1 for TON, MTW and MOR). Ds was computed as the mean value of five independent MD trajectories by fitting the MSD curve in the linear region, using a least-square fit.

3. Samples characteristics

3.1. Textural properties of Pt/H-form samples.

Table S1

Textural properties of Pt/H-form samples.

Sample	Surface area (m^2/g) [a]			Micropore Volume (cm^3/g) [b]
	S_{BET}	S_{mic}	S_{ext}	
Pt/H-ZSM-22(1)	214.8	166.1	48.6	0.08
Pt/H-ZSM-22(2)	198.7	165.9	32.8	0.08
Pt/H-ZSM-22(3)	187.5	162.6	24.9	0.08
Pt/H-ZSM-12(1)	308.6	205.8	102.8	0.10
Pt/H-ZSM-12(2)	299.6	199.7	99.9	0.10
Pt/H-ZSM-12(3)	300.2	196.5	103.8	0.10
Pt/H-MOR(1)	394.6	356.8	37.8	0.18
Pt/H-MOR(2)	376.5	328.0	48.4	0.16
Pt/H-MOR(3)	394.0	344.7	49.4	0.17

[a] Determined by the BET method.

[b] Calculated from the t-plot.

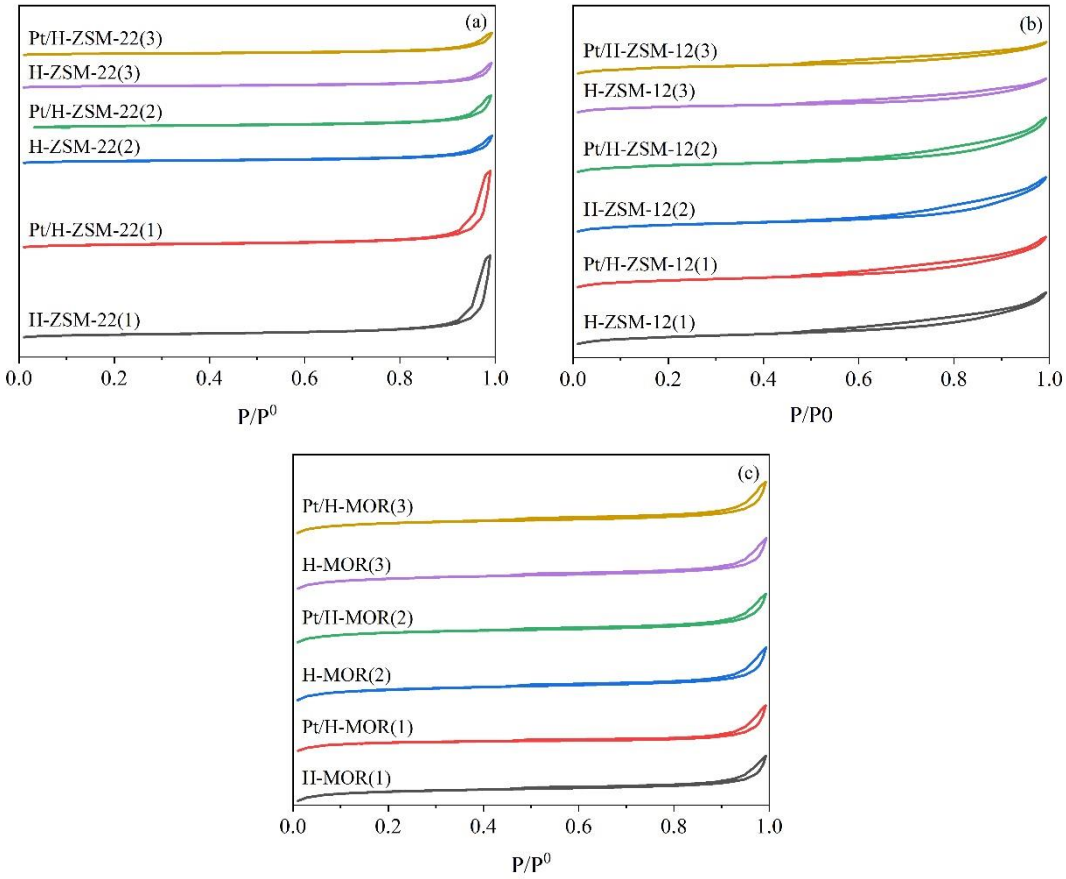

Fig. S2. N_2 adsorption-desorption isotherms of H- and Pt/H-form samples (a) ZSM-22, (b) ZSM-12, (c) MOR.

3.2. Acidity

Table S2

Acidity of different catalysts from NH_3-TPD

Sample	Acidity (μmol NH_3/g cat)		
	A_{Weak}	A_{Strong}	A_{Total}
H-ZSM-22(1)	89.2	98.2	187.4
H-ZSM-22(2)	85.3	94.8	180.1
H-ZSM-22(3)	80.0	89.3	169.3
H-ZSM-12(1)	82.2	95.5	177.7
H-ZSM-12(2)	75.3	86.5	161.8
H-ZSM-12(3)	67.8	74.6	142.4
H-MOR(1)	96.7	111.2	207.9
H-MOR(2)	84.4	92.6	177.0
H-MOR(3)	74.8	79.5	154.3

3.3. Metallic properties

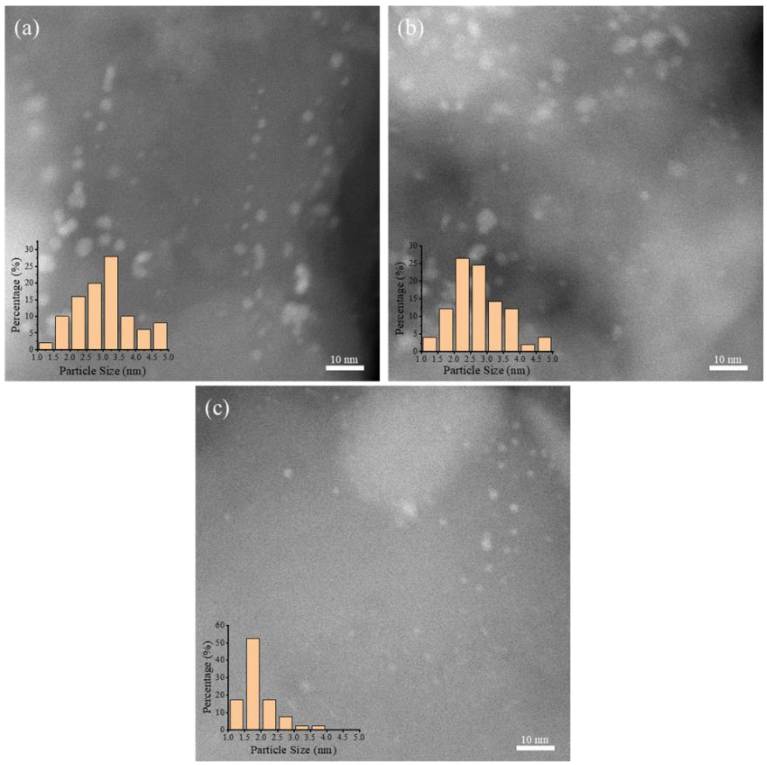

Fig. S3. TEM images of different samples (a) Pt/H-ZSM-22, (b) Pt/H-ZSM-12, (c) Pt/H-MOR.

4. Catalytic performance

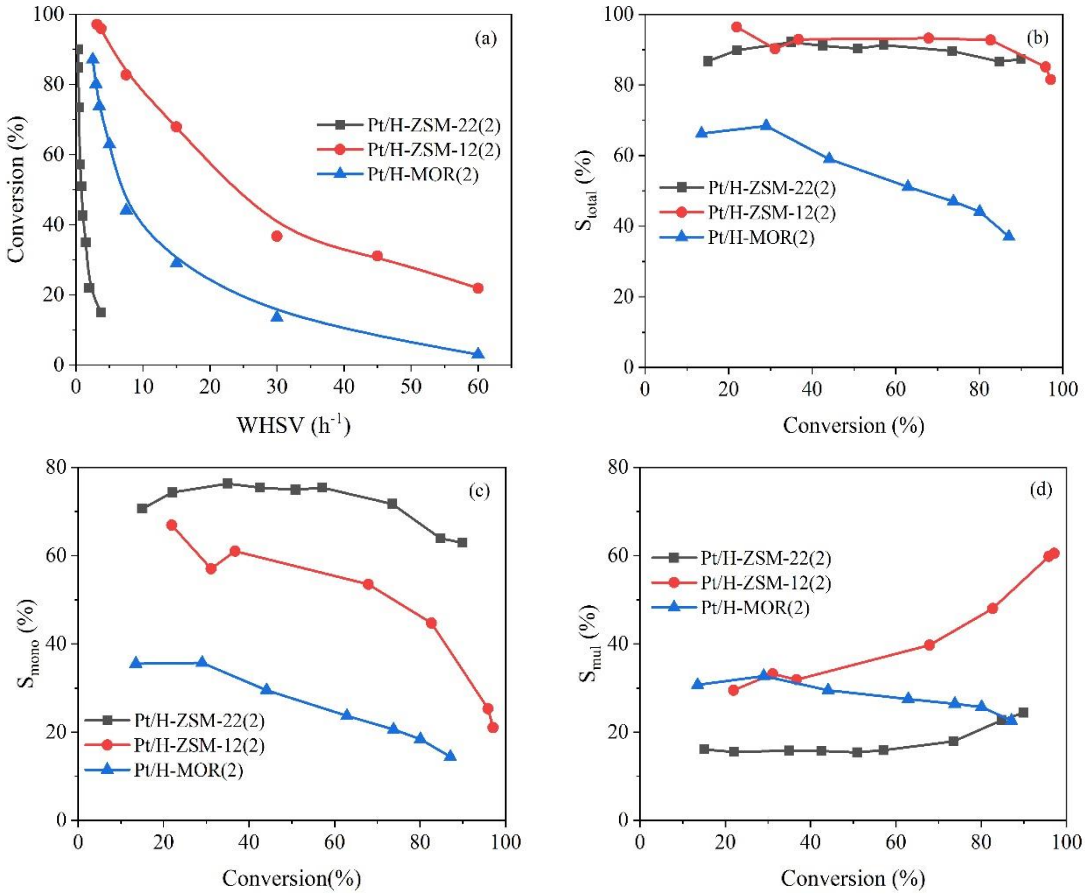

Fig. S4. The catalytic performance of Pt/H-ZSM-22(2), Pt/H-ZSM-12(2) and Pt/H-MOR(2) in n-dodecane hydroisomerization, (a) the conversion against the WHSV, (b) selectivity of total branched isomers versus conversion, (c) selectivity of mono-branched isomers versus conversion (d) selectivity of multi-branched isomers versus conversion. (Temperature = 280 ℃, H_2/n-C_{12} (mole) = 6, total pressure of 2.0 MPa.)

References

1. J. Yuan, Z. Liu, Y. Wu, J. Han, X. Tang, C. Li, W. Chen, X. Yi, J. Zhou, R. Krishna, G. Sastre and A. Zheng, *Proc Natl Acad Sci U S A*, 2021, **118**.
2. Baerlocher C and McCusker LB, Database of Zeolite Structures, http://www.iza-structure.org/databases/).
3. J. D. Gale and A. L. Rohl, *Mol. Simul.*, 2003, **29**, 291-341.
4. M. J. Sanders, M. Leslie and C. R. A. Catlow, *J. Chem. Soc., Chem. Commun.*, 1984, DOI: 10.1039/c39840001271, 1271-1273.
5. H. Sun, *The Journal of Physical Chemistry B*, 1998, **102**, 7338-7364.
6. D. Frenkel, B. Smit and M. A. Ratner, *Phys. Today*, 1997, **50**, 66-66.